Improved Genome Editing Efficiency and Flexibility Using Modified Oligonucleotides with TALEN and CRISPR-Cas9 Nucleases.

Jean-Baptiste Renaud, Charlotte Boix, Marine Charpentier, Anne de Cian, Julien Cochennec, Evelyne Duvernois-Berthet, Loïc Perrouault, Laurent Tesson, Joanne Edouard, Reynald Thinard, et al.

Cell Reports

Resource

Improved Genome Editing Efficiency and Flexibility Using Modified Oligonucleotides with TALEN and CRISPR-Cas9 Nucleases

Graphical Abstract

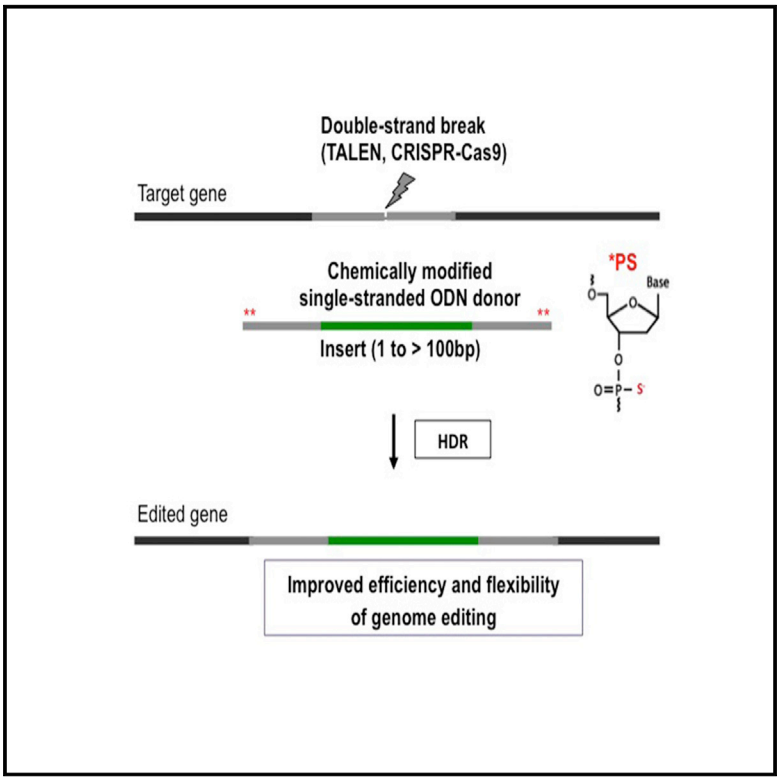

Highlights

- More-efficient genome editing with chemically modified oligonucleotide donors
- Greater flexibility with modified donors, allowing insertions more than 100 bp long
- Efficient mutant isolation in U2OS and RPE1 cell lines, as well as in rat and mouse
- Homozygous loxP site insertion at the mouse ROSA locus

Authors

Jean-Baptiste Renaud, Charlotte Boix, Marine Charpentier, ..., Ignacio Anegon, Jean-Paul Concordet, Carine Giovannangeli

Correspondence

jpconcordet@mnhn.fr (J.-P.C.), carine.giovannangeli@mnhn.fr (C.G.)

In Brief

Renaud et al. find that using chemically modified single-stranded oligonucleotide donors with CRISPR-Cas9 or TALEN nucleases enhances genome editing efficiency and flexibility in cell culture, rat, and mouse.

Renaud et al., 2016, Cell Reports *14*, 2263–2272
March 8, 2016
http://dx.doi.org/10.1016/j.celrep.2016.02.018

CellPress

Cell Reports
Resource

Improved Genome Editing Efficiency and Flexibility Using Modified Oligonucleotides with TALEN and CRISPR-Cas9 Nucleases

Jean-Baptiste Renaud,[1] Charlotte Boix,[1] Marine Charpentier,[1] Anne De Cian,[1] Julien Cochennec,[1] Evelyne Duvernois-Berthet,[1] Loïc Perrouault,[1] Laurent Tesson,[2,3] Joanne Edouard,[5] Reynald Thinard,[2,3] Yacine Cherifi,[4] Séverine Menoret,[2,3] Sandra Fontanière,[4] Noémie de Crozé,[5] Alexandre Fraichard,[4] Frédéric Sohm,[5] Ignacio Anegon,[2,3] Jean-Paul Concordet,[1,*] and Carine Giovannangeli[1,*]
[1]INSERM U1154, CNRS UMR7196, Museum National d'Histoire Naturelle, Paris 75005, France
[2]INSERM U1064, CHU de Nantes, Nantes 44093, France
[3]Platform Rat Transgenesis Immunophenomic, CNRS UMS3556, Nantes 44093, France
[4]genOway, Lyon 69007, France
[5]Amagen, CNRS UMS 3504, INRA UMS 1374, Institut de Neurobiologie A. Fessard, Gif-sur-Yvette 91198, France
*Correspondence: jpconcordet@mnhn.fr (J.-P.C.), carine.giovannangeli@mnhn.fr (C.G.)
http://dx.doi.org/10.1016/j.celrep.2016.02.018

SUMMARY

Genome editing has now been reported in many systems using TALEN and CRISPR-Cas9 nucleases. Precise mutations can be introduced during homology-directed repair with donor DNA carrying the wanted sequence edit, but efficiency is usually lower than for gene knockout and optimal strategies have not been extensively investigated. Here, we show that using phosphorothioate-modified oligonucleotides strongly enhances genome editing efficiency of single-stranded oligonucleotide donors in cultured cells. In addition, it provides better design flexibility, allowing insertions more than 100 bp long. Despite previous reports of phosphorothioate-modified oligonucleotide toxicity, clones of edited cells are readily isolated and targeted sequence insertions are achieved in rats and mice with very high frequency, allowing for homozygous loxP site insertion at the mouse ROSA locus in particular. Finally, when detected, imprecise knockin events exhibit indels that are asymmetrically positioned, consistent with genome editing taking place by two steps of single-strand annealing.

INTRODUCTION

Pioneer studies with I-Sce1 and zinc finger nucleases were used to establish the main principles of genome editing with sequence-specific nucleases (Porteus and Carroll, 2005). TALENs and even more spectacularly CRISPR-Cas9 have now hugely facilitated the design of sequence-specific nucleases to the target locus of interest, which is no longer the limiting step in genome editing (Hsu et al., 2014; Kim and Kim, 2014). When a double-strand break takes place, DNA repair usually proceeds with fidelity to the original sequence (Bétermier et al., 2014). However, when sequence-specific nucleases are used, mutations are introduced at high rates, possibly due to repeated cleavage and repair cycles until mutations disrupt cleavage site recognition. The DNA double-strand break repair pathways involved are thought to be mainly classical non-homologous end joining (NHEJ) and possibly alternative end joining (altEJ or MMEJ; Bae et al., 2014) that both mediate DNA ligation after processing of chromosomal ends. Other well-characterized pathways for DNA double-strand break repair are homology directed, for instance, homologous recombination using the sister chromatid during cell replication. For purposes of genome editing, donor DNA can be introduced into cells in order to program the sequence modification resulting from homology-directed repair. Several types of donor DNA have been used including plasmid DNA and synthetic oligonucleotides (Carroll and Beumer, 2014). Plasmid DNA with 1 kbp homology arms to sequence flanking the cleavage site is commonly used in gene-targeting experiments in mammalian cells. However, using CRISPR-Cas9 nucleases, it was found that homology arms longer than 1 kbp could stimulate gene-targeting efficiency by 2- to 4-fold (Chu et al., 2015), suggesting that specific optimization may be beneficial. Recently, DNA plasmids with very short homology arms, around 10 bp long, were shown to drive targeted insertion, likely by a MMEJ-based mechanism (Nakade et al., 2014). Single-stranded oligonucleotide (ssODN) donors have also been used successfully in many experimental systems, including cultured cells (Chen et al., 2011; Ran et al., 2013) and embryo injections (Beumer et al., 2013b; Harel et al., 2015; Paix et al., 2014; Shao et al., 2014; Tan et al., 2013). Stretches of homology to the sequence flanking the cleavage site are usually included in the ssODN design (Chen et al., 2011). In the mouse and rat, precise insertions and point mutations have been achieved at high efficiencies with ssODN donors (Yang et al., 2014; Yoshimi et al., 2014), whereas in zebrafish, extensive mutations of the ssODN or target site sequence were found in the great majority of insertions (Bedell et al.,

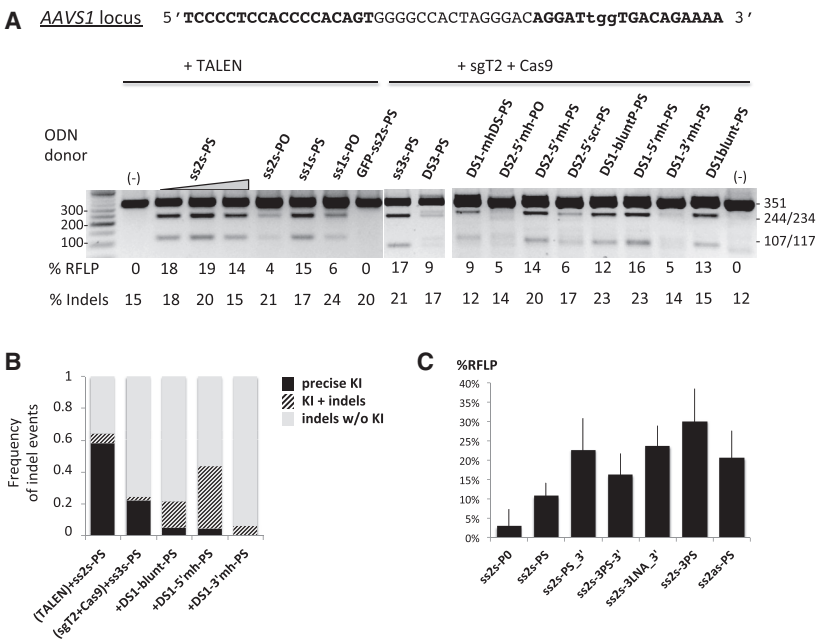

Figure 1. Optimization of Short ODN Donor Design

(A) Integration activity of short ss- and dsODN donors. TALEN target sequences (in bold) and PAM sequence (in lower cases) in an intron of the *PPP1R12C* gene within the chromosome 19 locus are shown. Single-stranded donor oligonucleotides (ssODNs) with short homology arms, ss1s (43-mer) and ss2s and ss3s (58-mer), and the 58-bp DS3 duplex (formed by hybridization of ss3s with its complementary strand) were used to make a sequence insertion including a PvuII site at the cleavage site. A control ssODN including a PvuII site but lacking homology arms, GFPss2s-PS, was also used. Double-stranded donors (dsODNs) (different versions of DS1 and DS2, as indicated) included an XhoI site (see sequences in Tables S1 and S2 and Figure S1). dsODNs containing microhomologous ends (DS1-mhDS-PS, DS1-5′mh-PS, DS2-5′mh-PS, DS2-5′mh-PO, and DS1-3′mh-PS) or not (DS1-blunt-PS, DS1-bluntP-PS, and DS2-5′scr-PS) were evaluated. RFLP analysis of DNA from U2OS cells treated with TALEN *AAVS1* or (sgT2+Cas9) and various ssODNs (at 12 μg, except ss2s-PS at 6, 9, and 12 μg) or dsODNs (at 12 μg) is shown. The corresponding rate of PvuII or XhoI cleavage (% RFLP) and of mutations evaluated in parallel by the T7 endonuclease I assay, T7E1 (indicated as % indels; gel not shown) are reported below the gel. PO, phosphodiester; PS, phosphorothioate. Fifty-base-pair DNA ladder (NEB) was shown. See also Figure S1 for integration activity of dsODNs.

(B) ssODNs, but not dsODNs, direct precise sequence insertions. The frequency of the different types of indels, evaluated by deep sequencing, are reported: % indels w/o KI (gray) and KI events that include the precise KI events (black) and KI with additional indels (hatched).

(C) Influence of location and nature of the modification in the oligonucleotide on genome editing efficiency. Different parameters were evaluated: the type of chemical modification (LNA [locked nucleic acid]), the number of modified nucleotides (two at both ends or at 3′ end in ss2sPS or ss2sPS_3′, resp.; three at both ends or at the 3′ end in ss2s-3PS or ss2s-3PS_3′ and ss2s-3LNA_3′, resp.). RFLP rate is shown for different modified oligonucleotides, as mean ± SD (3–20 independent experiments). For all the modified ssODNs compared to the PO ODN, p values from Mann-Whitney statistical analysis are <0.05. See also Figure S2 for impact of polarity of the PS-ssODN and of distance between break and gene edit (Figure S2A) and of homology length on activity of PO-ODNs (Figure S2B).

2012; Gagnon et al., 2014; Hruscha et al., 2013), therefore much limiting the use of ssODN donors in zebrafish.

We chose to more systematically test the potential of chemically modified ssODNs or double-stranded ODNs (dsODNs) for genome editing with sequence-specific nucleases. We investigate several parameters including the nature and location of modified bases, length of sequence insertion, and distance to cleavage site position. Different types of nucleases were tested, both TALENs and CRISPR-Cas9 nucleases, for genome editing in multiple experimental systems, including cultured cells and model organisms. Our results show that phosphorothioate (PS)-modified ssODNs exhibit improved efficiency and flexibility in most experimental systems tested. Interestingly, detailed analysis of gene edits reveals a variable proportion of imprecise sequence insertions, which could be due to different mechanisms of double-strand break repair by ssODNs.

RESULTS

Design and Activity of Short ss- or dsODN Donors

We first evaluated the homology-directed repair (HDR) capacity of ODNs with short homology arms. We tested both ssODNs and dsODNs to generate small insertions, and in each case, we evaluated different designs. ssODNs have been shown to be effective in genome editing, but several questions remain concerning how to optimize their design. Regular phosphodiester (PO) ssODNs of around 100 nucleotides (nt) long have been successfully used (Chen et al., 2011; Yang et al., 2013). We first tested chemically modified ssODNs for HDR. We started with the common PS modification, known to improve nuclease resistance (Eckstein, 2000). We designed ssODNs with short homology arms, ss1s, with 18 and 19 on each side of the break, and ss2s or ss3s, with 27 or 28 and 24 nt (see Table S1 for sequences). PS chemical modifications were incorporated at two terminal nucleotides of both 5′ and 3′ ends. Using *AAVS1* as a test locus, we introduced a PvuII restriction site sequence in ssODN (Figure 1A) for easy analysis of sequence insertion by restriction fragment length polymorphism (RFLP). We chose to insert the PvuII site directly into the expected cleavage site for the sequence-specific nucleases used here, *AAVS1*-specific TALEN with ss1s and ss2s and Cas9 combined with sgT2 guide RNA with ss3s. ssODN donors were co-transfected with *AAVS1*-specific TALEN or Cas9 and sgT2 guide RNA expression plasmids. Fourteen days post-transfection, the *AAVS1* locus was amplified by PCR and donor insertion into the *AAVS1* site assayed by PvuII digestion (Figure 1A). PS-modified ssODNs (ss1s-PS and ss2s-PS) directed robust sequence insertion efficiency in the presence of nucleases, whereas the corresponding unmodified ssODNs (ss1s-PO and ss2s-PO) led to only modest integration levels (6% versus 15% and 4% versus 14%, respectively). The knockin (KI) rates using PS-modified ssODNs were in the range of indel rates induced by nucleases at this site as measured by

the T7 endonuclease assay (T7E1), suggesting that the majority of modification events were donor-mediated insertions. A PS-ssODN including a PvuII site but lacking homology arms, ssGFPss2s-PS, did not induce any sequence insertion, as expected for an HDR-based mechanism. Finally, using the duplex version of the ODN donor (DS3) strongly decreased the integration rate (by 2-fold), consistent with a mechanism different from homologous recombination being involved for ssODNs.

Based on results showing that donors with microhomologies to the cleavage site ends can enable efficient integration of DNA fragments by MMEJ (microhomology-mediated end-joining) (Nakade et al., 2014; Orlando et al., 2010), we chose to evaluate the potential of dsODNs with microhomologies for integration at the Cas9 cleavage site directed by guide RNA sgT2. Based on the fact that cleavage sites are processed during repair, generating different types of DNA ends (Dorsett et al., 2014), we tested different types of microhomologous ends, either double-stranded (mhDS), single-stranded 3′ overhangs (3′mh), or single-stranded 5′ overhangs (5′mh) (see sequences in Figure S1 and Table S2). As above, two PS nucleotide residues were included at 5′ and 3′ ends of dsODNs and the sequence insertion consisted of an exogenous 40- or 46-bp sequence (DS1 or DS2, respectively) including an Xho1 restriction site. Control donor oligonucleotides were used that had either no homology (DS1-blunt-PS and DS1-bluntP-PS; a 5′ phosphorylated version of the former) or 8 nt 5′mh predicted not to base pair with the sequence at the cleavage site (DS2-5′scr-PS). These dsODN donors were co-transfected with Cas9 and sgT2 guide RNA expression plasmids. Six days post-transfection, the *AAVS1* locus was amplified by PCR and sequence insertion into the *AAVS1* site assayed by XhoI digestion (Figure 1A). As observed with ssODN donors, the PS modification strongly enhanced integration of duplex donors (14% compared to 5% for DS2-5′mh-PS and -PO, respectively). Sequence insertion was observed for all the designs tested but at different rates (Figure S1B). In particular, as recently reported, dsODN with blunt ends integrated at frequencies corresponding roughly to 1/2 indel mutation rates (Tsai et al., 2015). Importantly, the duplex with the non-complementary overhangs (DS2-5′scr-PS) also led to XhoI sequence insertion. These results were confirmed at another cleavage site, at the *SOD1* gene (Figure S1C). At this target, blunt and overhang-containing duplexes also led to targeted donor sequence insertion regardless of the presence of microhomologous ends (4% and 9% for DS2-sod5′mh-PS and DS2-sod-3′mh-PS, which had microhomologous ends, compared to 7% and 11% for DS2-5′mh-PS or DS1-blunt-PS, without), indicating that there is no need for microhomologous ends to achieve efficient integration. This finding suggested that imprecise sequence insertions were taking place.

ssODNs, but Not dsODNs, Direct Precise Sequence Insertion

To determine the fidelity of donor sequence insertion, the PCR amplicon from the *AAVS1* target was subjected to deep sequencing. For ssODNs, the majority of insertion events were precise (representing more than 90% of total KI events) and only a low frequency of imprecise insertions was detected (indicated as "KI+indels" with hatched bars; representing less than 10% of total KI events; Figure 1B). With the short duplex donors, sequence information in the microhomology arms was expected to result in precise donor sequence insertion without loss of either chromosomal or donor sequence. However, only few integration events were precise. Poor efficiency of precise insertion could be due to insufficient levels of available complementary "acceptor" ends after target sequence cleavage by Cas9, which is known to generate blunt ends (Jinek et al., 2012). Recent studies using TALENs or CRISPR-Cas9 and DNA plasmid donors containing microhomologies, although demonstrating precise MMEJ-based integration, also exhibited significant amounts of imprecise integration events (Nakade et al., 2014). In contrast, previous studies that showed efficient precise insertion with dsODN donors carrying microhomologies were performed with zinc finger nucleases that generate 5′ protruding ends (Orlando et al., 2010).

Chemical Modifications of ssODNs Stimulate Genome Editing

Based on the sequencing data, we next focused on ssODNs donors that were the most efficient for precise sequence insertion. We evaluated a set of ssODNs in order to determine parameters impacting genome editing efficiency. We first performed experiments to assay the importance of the nature and location of chemical modifications. PS modifications were positioned at both ends, as above, or at 3′ end only, and we compared efficiency of two to three PS-modified nucleotides. In addition to PS modification, we selected LNA, locked nucleic acid, known to improve ODN chemical and thermal stability (Jepsen and Wengel, 2004). Donor insertion into the *AAVS1* site was assayed as described above by RFLP analysis. All the chemically modified donors strongly enhanced donor sequence insertion compared to the PO-ssODN donor (Figure 1C). These data are consistent with a model in which ssODN end modifications enhance intracellular stability, thus enabling increased efficacy of genome editing.

Because chemical modifications, especially PS, have been described to be toxic (Rios et al., 2012), we carefully investigated the long-term survival and proliferation of modified cells. Sequence insertion rates were found to remain unchanged up to 15 days after treatment, whether using an ssODN containing PS modifications or standard PO chemistry.

We designed ssODN donors of variable sense and antisense orientations (s and as). At the *AAVS1* locus, the antisense donor, ss2as-PS, used with the *AAVS1*-specific TALEN, was slightly but significantly more efficient than the sense donor, ss2s-PS (Figure 1C; $p = 0.008$ from Mann-Whitney statistical analysis). However, in all the situations that we have tested (for example: *AAVS1* locus in Figure S2A; *GFP* transgene in Figure S4C), both orientations worked, sometimes with slightly different efficiencies, but no general rule emerged for sense or antisense orientation preference.

Improved Flexibility of Genome Editing Using PS-ssODN Donors

We next investigated the effect of homology length on gene editing in the context of ssODN donors and assayed targeted sequence insertion at the *AAVS1* locus (Figure S2B). In previous

work using PO-ssODNs, lengths in the range of 100 nt were common in most applications. We compared the ss1, ss2, and ss95 donors with 37, 51, and 84 nt total homology regions, respectively. As already shown in Figure 1A, short ss1-PO and ss2-PO donors drive limited donor sequence insertion compared to their PS counterparts. Using longer PO donors with an 84-nt total homology ss95-PO can strongly improve the activity compared to 51 nt (22% for ss95-PO compared to 5% for the same concentration of ss2-PO; Figure S2B). This observation was confirmed on *SUFU* gene, extending from a 73- to a 97-nt total homology region (43% for Sufu-1FLAG-L-PO versus 12% for the same concentration of Sufu-1FLAG-PO; Figure S2B). Although unmodified PO-ssODNs are intrinsically less efficient than chemically modified ones, using longer PO donors at high concentrations can compensate for their lower activity, possibly because sufficient homology is preserved from exonuclease degradation to maintain activity. However, lengthening of the homology above 90–100 nt has been described to be detrimental (Yang et al., 2013), likely because it could be prone to secondary structures decreasing the amount of donor effectively available for gene editing. In addition, using long homologous regions limits the size of functional sequences that can be inserted because chemical synthesis allows robust production of ssODNs no longer than 200 nt.

When using ssODN donors for sequence insertion, DNA cleavage is commonly designed to take place less than 10 bp away from the desired insertion site (Yang et al., 2013). In experiments described above, we designed the ssODN donors (ss1, 2, and 3) to make the insertion exactly at the expected cleavage site. We therefore wanted to examine in more detail how the rate of sequence insertion varies with its distance to the cleavage site. We tested a combination of nuclease and ssODN donor pairs (TALEN, sgT2, sgU2, and sgS1 and ss2, ss2L, and ss4; Figure S2A), generating DSBs at various distances from the insertion position. Here, we observed robust efficiency for sequence insertions at distances from 8 to 20 bp (Figure S2A), further establishing the flexibility of ssODN design when using PS modifications.

Efficient Gene Tagging with a 102-bp Insert Using PS-ssODNs

To demonstrate the general applicability of our results, we further tested similar reagents at different genomic loci and cell lines. The optimized ODN design was tested on different genes in Hedgehog signaling, a major signaling pathway in development and oncogenesis. We sought to introduce FLAG-tag coding sequences as a typical application of genome editing that should facilitate functional characterization of proteins for which antibody resources are limited. First, different amounts of PS- and PO-ssODNs were co-transfected in U2OS cells with TALENs targeting the ATG start codon of the SUFU protein coding sequence. Interestingly, as shown at the *AAVS1* locus, PS-ssODNs resulted in higher efficiency of FLAG-tag sequence integration (36% for Sufu-1FLAG-PS compared to 12% for -PO for example at the higher dose and 27% versus 1% at the lower dose; Figure 2A). The insertion size is limited by ODN synthesis capacity and length of homology arms. Considering that we can use shorter homology sequences by including PS modifications, we tested whether PS- ssODN would allow making longer sequence insertions. As shown in Figure 2A, we found that using PS-modified ssODN allowed very efficient insertion of more than 100 bp whereas only limited integration could take place with non-modified ssODN (53% for Sufu-3FLAG-HA-PS versus 3% for -PO), demonstrating a striking advantage of modified compared to non-modified ssODNs. To further generalize our findings, we tested insertion of FLAG-tag coding sequences in a series of genes of the Hedgehog signaling pathway (*SUFU*, *GLI2*, *GLI3*, *MLF1*, *SMO*, and *KIF7* genes) in U2OS cells and in a non-transformed RPE1 human cell line (Figure 2B). Efficient insertion could be induced at all loci tested by co-transfection of modified ssODNs with TALENs targeting the corresponding sequences. In the absence of TALEN co-transfection or when using control oligonucleotide with no sequence homology to the target, we could not detect FLAG-tag coding sequence integration by PCR. We further exploited the use of short modified ssODNs to evaluate the FLAG-tag insertion at two genes simultaneously. Transfection of the corresponding pairs of nucleases and donors gave rise to efficient insertion at both targets (*SUFU* and *GLI2* genes; Figure S2C). When comparing results between the two cell lines, we observed that KI rates were higher in U2OS (KI rates ranging between 20% and 50%) than in RPE1 cells (KI rates ranging from 2% to 12%; Figure 2B), possibly due to differences in nuclease cleavage efficiencies and/or intrinsic differences in activities of DNA repair pathways. Importantly, in RPE1 cells, KI events at all loci tested could only be easily detected with PS- and not PO-ssODNs donors (for example, 5% for Sufu-1FLAG-PS versus 0% for -PO and 4% for Sufu-3FLAG-HA-PS versus 1% for -PO; Figure 2B, lower panel).

Efficient Isolation of Tagged Cell Clones with PS-ssODNs

We next examined whether cells carrying the genome edits of interest could be isolated. Given the high frequencies of genome editing observed (see Supplemental Experimental Procedures), we seeded cells at clonal density and directly isolated and analyzed a series of clones. Targeted genome editing was analyzed at the DNA and protein levels. We could readily isolate clones carrying the integration of tag-coding sequences either at one or at multiple alleles in U2OS and in RPE1 cells (Figure 2C). The rate of KI alleles in the clones analyzed was roughly equivalent to the KI rates measured in the initial cell population, therefore supporting the absence of specific toxicity of PS-ssODNs. Fewer positive clones were isolated in RPE1 cells, as expected from the lower genome editing efficiency compared to U2OS cells. At the protein level, it was possible to detect tagged SUFU proteins with anti-FLAG antibody in positive clones from both cell lines, with the expected signal amplification for the clones containing the 3FLAG-tagged Sufu protein compared to 1FLAG-tag. The readily achieved isolation of modified clones showed that treatment of cells with PS-modified ODNs was compatible with long-term expansion of modified cells.

Successful KI in Rat, Mouse, and Zebrafish with PS-ssODNs

We next wanted to examine the potential of modified ssODNs in genome editing of model organisms, both testing the benefit of modified ssODNs compared to PO-ODNs and further checking

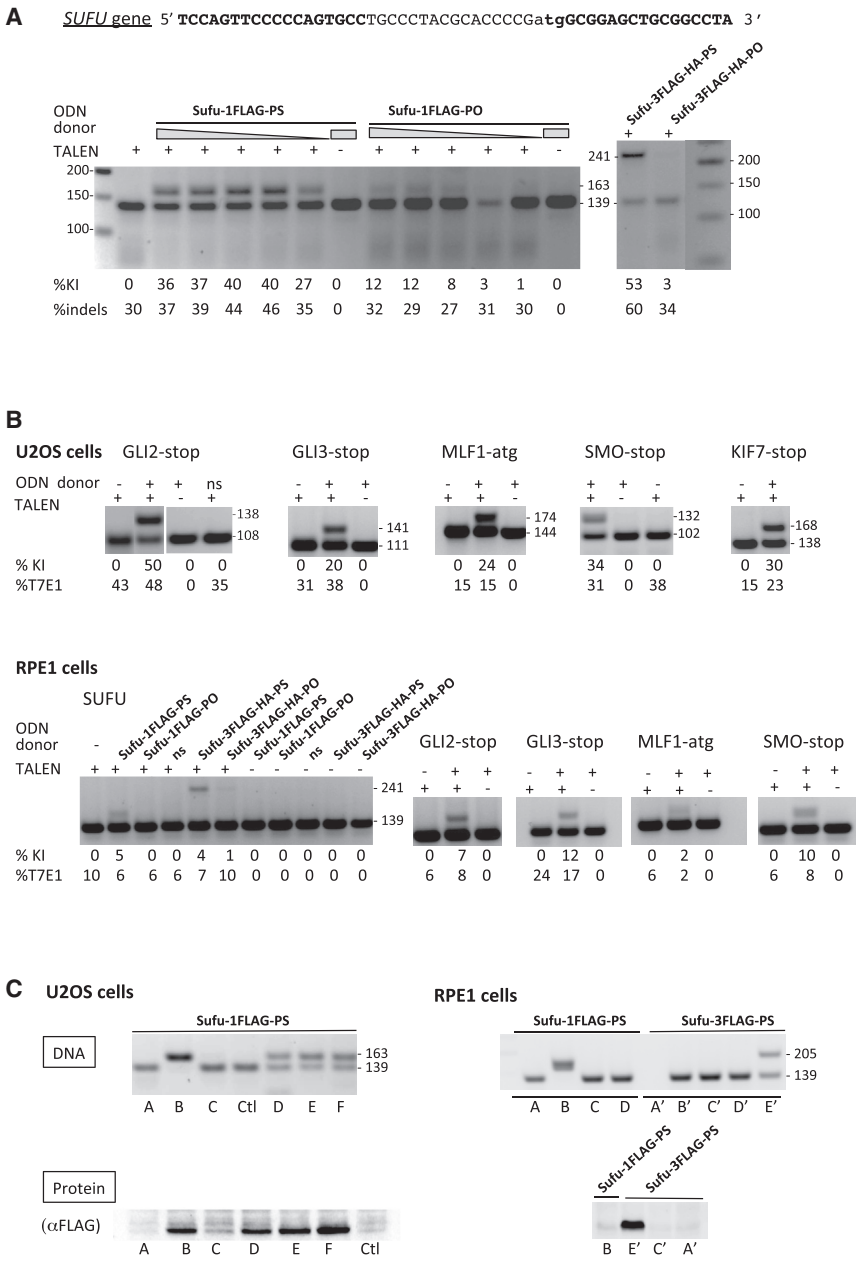

Figure 2. Efficient Tag Sequence Insertion of More Than 100 bp Using Modified ODNs at Genes of the Hedgehog-Signaling Pathway

TALENs and ssODNs were designed to perform insertion of FLAG-tag coding sequences at the ATG or STOP codon positions of the indicated genes in the Hedgehog-signaling pathway. DNA was extracted and PCR amplified to evaluate the efficiency of FLAG-tag sequence insertion and perform the T7E1 assay. % KI indicates the relative abundance of the higher size band corresponding to FLAG-tag sequence insertion relative to the total DNA bands. % indels indicates the mutation rates calculated from the T7E1 assay results and %T7E1 the cleavage rate by T7E1 (gel not shown). Note that, when provided, indels rates were calculated by taking into account the KI population, as detailed in Experimental Procedures.

(A) SUFU gene tagging in U2OS cells. TALEN target sequences (in bold) around the start codon (lower cases) of the SUFU gene are shown. ssODNs containing insertion of one FLAG-tag sequence (24 bp), Sufu-1FLAG-PS, and Sufu-1FLAG-PO or 3FLAG-HA sequence (102 bp), Sufu-3FLAG-HA-PS, and Sufu-3FLAG-HA-PO were used at different doses with TALEN expression plasmid (for Sufu-1FLAG-PS and Sufu-1FLAG-PO: 15, 12, 9.6, 7.2, and 4.8 μg or 15 μg with ssODN alone; 6 μg for Sufu-3FLAG-HA-PO and Sufu-1FLAG-PS). Fifty-base-pair DNA ladder is shown on the right.

(B) Targeting of Hedgehog-signaling genes in U2OS and RPE1 cells. PS-ssODNs containing one FLAG-tag coding sequence were used (see Table S1 for sequences). Transfection was performed with TALEN expression plasmids and/or ssODNs (12 μg), as indicated. ns indicates control ssODN lacking homology arms. For Smo-FLAG-PS, we could initially detect products corresponding to potential FLAG-tag sequence integration in the absence of nucleases but realized that this was due to PCR artifacts, and special care was taken to exclude PCR artifacts, which included using DNA extracted 3 weeks after transfection and treating DNA samples with single-strand DNA nucleases before PCR (Figure S3). See also Figure S2C for multiplex tag sequence insertion.

(C) Efficient isolation of clones with FLAG- or 3FLAG-tagged SUFU gene from cells treated with PS-modified ssODNs. Cell clones were isolated after transfection with SUFU-specific TALEN expression plasmids and the indicated PS-ssODNs. Uppercase labels indicate specific clones analyzed at both DNA and protein levels; Ctl lane corresponds to untreated cells. Protein expression was analyzed by western blot using anti-FLAG antibody. See also Figure S4 for successful ssODN-mediated KI in rat, mouse, and zebrafish.

for toxicity. In the rat and mouse, it was previously reported that non-modified ssODNs with long homology arms can direct efficient sequence insertion during repair of double-strand breaks induced by TALEN or CRISPR-Cas9 nucleases whereas, in the zebrafish, only modest levels of precise sequence insertion could be achieved (Bedell et al., 2012; Gagnon et al., 2014).

For tests in the rat, we targeted the *Cftr* gene. ssODNs were designed with 45-nt homology arms flanking a single A nt that creates a XbaI restriction site for facile genotyping of *Cftr* mutant rats and that simultaneously disrupts the open reading frame of the *Cftr* gene and target sequence of the guide RNA (to prevent cleavage of the successfully edited genomic sequence; Figure S4A). The genome editing strategy was first tested in cultured rat C6 glioblastoma cells. In line with results described above, successful insertion, although at very low levels, could be detected when guide RNA and Cas9 expression plasmids were co-transfected with PS-ssODN, but not with PO-ssODN (Figure S4A). PS- or PO-ssODNs were next co-injected with guide RNA and Cas9 mRNA into rat fertilized zygotes. Rat pups born from the injections were genotyped by PCR and XbaI digestion as well as by DNA sequencing. Embryo viability and newborn frequencies were in a similar range with PS- and PO-ssODNs,

Table 1. Efficient Genome Editing with PS-Modified ssODNs in Model Organisms

Target Locus	ssODN Donor	Cas9/sg/ssODN (ng/μl)	No. of Newborns	No. of E15	No. of KI (%)	No. of NHEJ (%)
Rat *Cftr* gene	PS	20/10/15	23	–	6 (26.1)	9 (39)
		50/10/15	41	–	13[a] (31.7)	22 (53.6)
	PO	20/10/15	49	–	13[a] (26.5)	31 (63.3)
		50/10/15	65	–	15[b] +1[c] (24.6)	34 (52.3)
Mouse *ROSA 26*	PS	20/10/25	–	8	3[d] +2[e] (62.5)	4 (50)
	PO	20/10/25	–	21	2 (9.5)	15 (71.4)

(Top) Genome editing with PS- and PO-ssODNs in rat. Two series of injections into rat fertilized oocytes were performed, loading injection pipettes with a solution containing *Cftr* guide RNA, Cas9 mRNA, and *Cftr* PS- or PO-ssODN as indicated (sequence information is provided in Figure S4A). Tail DNA was extracted from newborns, and targeted modification of the *Cftr* gene was examined by PCR and XbaI digestion to quantitate the insertion efficiency (Figure S4A), as well as by PCR and high-resolution DNA capillary electrophoresis to quantitate indel mutations. Quantifications and sequence modifications were confirmed by DNA sequencing of PCR products. Rats that are heterozygotes with one KI and one NHEJ event are included in both KI and NHEJ animal counts indicated in the table. See also Figure S4A.

(Bottom) Genome editing with PS- and PO-ssODNs in mouse. Injection was performed in mouse oocytes with a solution containing *Rosa* guide RNA, Cas9 mRNA, and *Rosa*-PS- or PO-ssODN as indicated (see experimental design in Figure S4B). DNA from E15 embryos was extracted, and insertion of loxP sequence was analyzed by PCR and BglII digestion to evaluate insertion rate (Figure S4B) and confirmed by sequencing of PCR products. Mice that are heterozygotes with one KI and one NHEJ event are included in both KI and NHEJ animal counts indicated in the table. See also Figure S4B.

[a]Including one homozygous KI animal.

[b]Including four homozygous KI animals.

[c]All KI events corresponded to precise sequence insertion, except for one KI obtained with the PO-ssODN, which showed a double copy of ODN sequence.

[d]Including three homozygous KI mice.

[e]The insertion events are precise for all embryos except two: one that had a 137-bp deletion on the 5′ side of the insert and the other two point deletions, one on each side of the insert.

indicating that no specific toxicity was associated with PS- compared to PO-ssODNs (Figure S4A). Strikingly, a high proportion of embryos carried the wanted sequence insertion when either type of ssODN was injected: 24.6%–31.7% of newborns were KI-positive, and in several rats, KI was detected on both alleles. All rats with KI events showed precise integration of the ssODN, irrespective of the type of ssODN, with the exception of one rat that showed integration of two ssODN sequences in tandem after injection of PO-ssODN. NHEJ events were frequent in all experimental groups (39%–63.3% of newborns), attesting high efficacy of the guide RNA. In addition, we evaluated the specificity of ssODN integration using the targeted locus amplification (TLA) method (de Vree et al., 2014), which allows to define the genomic integration site of a given exogenous sequence. The integration sites of the ssODN donor were mapped by TLA in a rat that had been found to have precise KI at the *Cftr* locus. TLA showed integration of the ssODN at the *Cftr* locus, as expected, and not at any other genomic site, demonstrating that only specific ssODN integration had taken place.

In the mouse, the ssODN was designed to insert at the ROSA locus a 34-bp loxP sequence, a genome edit of high interest to generate alleles for conditional gene inactivation with the Cre-loxP system (Branda and Dymecki, 2004), and a BglII site to facilitate genotyping (Figure S4B). Zygotes injected with PS- or PO-ssODN donors were genotyped at the blastocyst stage (Figure S4B) or at E15 (Table 1). In contrast to the results at the rat *Cftr* locus, co-injection of PS-ssODN led to a much-higher efficiency of sequence insertion (62.5% versus 9.5% with PO-ssODN). Notably, several E15 embryos carried KI at both alleles when using PS-ssODN whereas none was found with PO-ssODN. In both groups, the rates of NHEJ-modified mice were comparable (50% and 71.4%). As observed in rats, survival rates were equivalent with the PS- and the PO-ssODN donors (Figure S4B). Because the experimental injection setup and initial stages of mouse and rat embryo development are highly similar, it was surprising that the benefit of PS-ssODNs was much more dramatic in the mouse. One possibility is that PS-ssODNs were much more efficient because the sequence edit was much longer in the mouse experiment, a 40-nt insertion compared to 2-nt deletion in the rat, and insertion of long sequences is likely less efficient, making the PO-ssODNs suboptimal.

Finally, we tested PS-ssODNs targeting a *GFP* transgene in zebrafish. After co-injection of PS-ssODN with GFP-specific TALEN proteins, GFP-negative embryos were analyzed individually for sequence modification at the target locus by deep sequencing. As previously reported with PO-ssODNs, only very low levels of precise donor sequence insertion were obtained (Figure 3A). In one embryo (E8), however, a high proportion of precise donor insertion was detected, likely due to insertion at early cleavage stages. Although PS-ssODN did not allow to improve the rate of precise sequence insertion in zebrafish embryos, one embryo exhibited sufficient levels of precise KI to expect germline transmission.

Indels Found in Imprecise KI Are Asymmetrically Positioned

The detailed analysis of sequences corresponding to imprecise KI in zebrafish exhibited some specific characteristics. We observed that in a large majority of cases, the sequence modifications (relative to the expected, precise KI) were located on the 5′ side of the 7-bp insert (Figure 3A). Asymmetry was also noted in some imprecise KI events resulting from using PO-ssODNs

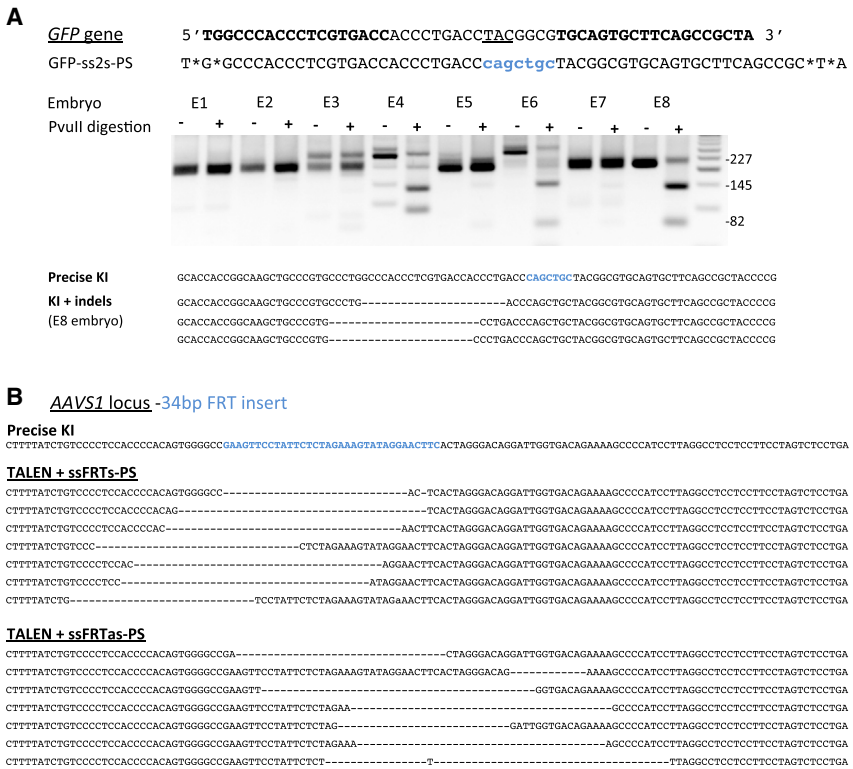

Figure 3. Nature of Imprecise KI Events Using Sequence-Specific Nucleases and ssODNs

(A) Test of genome editing with PS-modified ODNs in zebrafish. (Upper panel) TALEN target sequences (in bold) around the fluorophore-specific codon of the *GFP* gene (underlined). A PS-ssODN, carrying two phosphorothioate linkages at both 5′ and 3′ ends, was designed to introduce a 7-bp sequence including a PvuII site (in blue lowercase) into GFP cDNA, resulting in frame shift and GFP inactivation. Preliminary transfection experiments were conducted in cells stably expressing GFP to demonstrate that efficient GFP inhibition could be induced by co-transfection of GFP-specific TALENs together with PS-ODNs and GFP-ss2-PS (Figure S4C). (Middle panel) The PS-ssODN was co-injected together with GFP-specific TALEN proteins into one-cell-stage zebrafish embryos carrying a ubiquitously expressed *GFP* transgene, and GFP-negative transgenic embryos were identified. Single GFP-negative embryos (E1–E8) were lysed in PCR buffer and the *GFP* target sequence amplified and PvuII-digested to evaluate the insertion efficiency. (Lower panel) Genotyping was performed by deep sequencing of PCR products. The three most-frequent sequences corresponding to imprecise KI (KI+indels) in E8 embryos are shown with the expected KI sequence (Precise KI) reported on the top as a reference (insert in bold blue).

(B) Examples of imprecise KI events obtained in U2OS cells. The most-frequent imprecise KI products are shown for U2OS cells treated with TALEN targeting the *AAVS1* locus in the presence of the ssFRTs-PS or ssFRTas-PS donors that were designed to introduce a 34-bp-long FRT insert sequence (insert in bold blue).

In (A) and (B), imprecise KI sequences correspond to FRT insertion exhibiting additional indels on the 5′ side of the insert sequence, referring to the ssODN sequence orientation.

with TALENs in zebrafish (Bedell et al., 2012). We therefore examined in more detail the imprecise insertions detected previously in U2OS cells treated with ssODNs. We analyzed DNA of cells treated with guide RNA sgT2 and ss3s-PS or ss3as-PS, or with TALEN and ss2s-PS or ss2as-PS, and we focused on sequences including indels in addition to the insert sequence 5′-cagctg-3′. We observed that there is an asymmetry in the location of indels: they are mainly located on the 5′ side of the edit with ss3s donor as in zebrafish and on the 3′ side for the ss3as donor. In other words, referring to the ssODN sequence, indels are always present on the 5′ side of the insert in the ssODN sequence (Table 2). In order to further analyze imprecise insertion events, we also sequenced the *AAVS1* target locus after treatment with *AAVS1*-specific TALEN and an ssODN donor designed to introduce a 34-bp-long FRT sequence. In a majority of cases, imprecise insertions exhibited either indels at the *AAVS1* sequence next to the complete insert sequence or partial FRT sequence insertions with deletions of the insert and adjacent *AAVS1* sequence. In both cases, indels were asymmetrically localized, being predominantly on the 5′ side (referring to the ODN sequence; Figure 3B; Table 2). Other types of imprecise KI (exhibiting indels on the 3′ side or more-complex insertion events) were observed in much-lower proportions. It is interesting to note that, compared to ss2 or ss3 donors, imprecise KI events were slightly more frequent for the FRT donor, which corresponds to insertion of a longer sequence and could be more error prone. In rat, all KI events obtained with PS-ssODN were precise, whereas in mouse, two out of five KI included indels. The results reported are consistent with a model for ssODN-mediated genome editing dependent on two steps of single-strand annealing, as proposed in yeast (Storici et al., 2006), which is shown in Figure S5 and further discussed below.

DISCUSSION

Here, we demonstrated that chemically modified ssODNs provide several important benefits to the design of ssODN donors for genome editing. Remarkably, we showed that the use of PS-ssODN donors can give rise to much-higher levels of KI, especially for long inserts, both in cells and in rodents. Chemical modifications, PS or LNA, stabilize ssODNs and probably contribute by increasing the effective concentration of ssODN available during DNA repair. Recently, chemically modified guide RNAs were also demonstrated to improve genome editing (Hendel et al., 2015), and chemical modification of different types of linear donors used in genome editing (Sargent et al., 2011) might also be beneficial, as shown here for short ss and dsODNs. PS-ssODNs have been documented to be toxic or inhibit cell proliferation (Rios et al., 2012), but we found here, however, that isolation of cells, mouse embryos, and newborn rats with

Table 2. Asymmetry of Indels Found in Imprecise KI in U2OS Cells

			% Imprecise KI	
	Total Reads	% Precise KI	% KI + 5′ Indels	% KI + Other Indels
sgT2+Cas9+ss3s-PS	169,890	11.2	1.1	–
sgT2+Cas9++ss3as-PS	154,707	8.1	1.2	0.1
TALEN+ss2s-PS	13,748	14.7	1.5	–
TALEN+ss2as-PS	32,186	15	1.8	0.6
TALEN+ssFRTs-PS	106,778	20.8	5	0.1
TALEN+ssFRTas-PS	88,714	18.9	3.1	0.1

The percent of DNA target sequences with precise insertion (precise KI) and imprecise insertion exhibiting indels on the 5′ side of the insert, referring to the ssODN sequence orientation, (KI + 5′ indels) or other types of indels (KI + other indels) were evaluated by deep sequencing and are indicated for different pairs of nucleases and ssODNs, corresponding to either target sequence orientation (s or as). In all cases, the large majority of imprecise KI sequences exhibit additional indels on the 5′ side of the insert sequence, except in the case of TALEN+ss2as-PS. In the latter case, additional indels were likely induced by a second step of DNA cleavage by TALENs and NHEJ repair after an initial precise KI event. Indeed, the 7-bp insert resulted in a 22-bp-long spacer between the two TALEN-binding sites that still allowed for DNA cleavage by TALENs (as checked in vitro; not shown) and generation of additional indels after precise KI.

targeted sequence insertion is readily achieved. Concerning the homology length, we showed that as short as 20 nt on each side of the break is sufficient when using PS-ssODNs. Including modified nucleotides in the donor therefore allows to decrease the homology length while maintaining activity and therefore significantly increases design flexibility. The main advantage is to be able to make longer sequence insertions. Here, a sequence insertion of more than 100 bp could be achieved, allowing the insertion of multiple tags that are useful for protein functional analysis. In ssODN design, the distance between the insertion and cleavage sites is also an important parameter that may benefit from ODN chemical modification because, in practice, cleavage sites are limited to sequences adjacent to NGG or NGA PAM motifs of *S pyogenes* Cas9 and its VQR variant, respectively (Kleinstiver et al., 2015; Zetsche et al., 2015). We found that a distance of 20 bp still allows for very efficient sequence insertion with PS-ssODN.

Concerning the specificity of integration events, we used the recently described approach, TLA (de Vree et al., 2014), to uncover potential off-target insertion sites. Analyzing one KI rat, we observed no insertion of the ssODN outside of the targeted loci, demonstrating specificity. ssODN integration seems to be a highly specific process because it needs both genomic cleavage and homologous regions, allowing stable base pairing near the break.

In addition to ssODNs, we also evaluated short microhomology-containing duplex donors and showed that chemically modified duplexes also exhibit increased insertion activity. However, very poor levels of precise KI were obtained. Enhancement of MMEJ repair pathways or reduction of NHEJ and better understanding of the mechanisms involved in microhomology-based duplex insertion might increase the precision of sequence insertion and reduce NHEJ-dependent sequence modifications. Using the recently described RNA-guided nuclease Cpf1, which generates 5′mh, instead of Cas9 could also improve the precision of insertion events by providing more-appropriate "acceptor" ends (Zetsche et al., 2015).

With ssODN donors, the insertion events are mostly precise in many biological systems, such as human cell lines or rodents, as reported here. In contrast, in zebrafish, imprecise KI events are predominant. In the latter case, phenotypic screening was performed here with GFP and made it possible to identify embryos with the wanted sequence insertion by screening a limited number of embryos. Phenotypic screening could also be performed at a control pigmentation locus, easily targeted in parallel to the locus of interest by co-injection of specific guide RNA, in order to select for embryos where genome modification efficiently took place and help limit the number of animals to be raised and screened.

ssODN-mediated genome editing is likely not mediated by the classical homologous recombination pathway, which involves double-stranded DNA template during repair (Majumdar et al., 2008; Storici et al., 2006). Based on our analysis of sequences from imprecise KI events, we propose that genome editing with ssODN takes place by two steps of single-strand annealing as proposed in yeast (Figure S5; Storici et al., 2006), and it will be interesting to test the direct contribution of components of the single-strand annealing (SSA) pathway. Better understanding the factors underlying ssODN-based genome editing and cross-regulations between DNA repair pathways may help to stimulate genome editing efficiency in different cellular contexts, as shown in *Drosophila* (Beumer et al., 2013a) or more recently in mouse embryos, where LIG4 inhibition allowed to favor KI events (Chu et al., 2015). In conclusion, we propose here an optimized KI approach based on PS-modified ssODN donors and validate its improved activity in different biological systems, both in cultured cells and in vivo. Such scalable and robust approach should be useful for precise sequence manipulation, expanding the versatility and applicability of genome editing with sequence-specific nucleases.

EXPERIMENTAL PROCEDURES

Plasmid, oligonucleotide, RNA, and TALEN materials are detailed in Supplemental Information.

Cell Transfection

The human cell lines U2OS, RPE1, and rat C6 cells (ATCC) were nucleofected (5×10^5–10^6 cells; kit V [Lonza] and Amaxa program X-001) with 2 μg of each TALEN or 2 μg of each Cas9 and guide RNA plasmids.

Microinjections into Rat, Mouse, and Zebrafish One-Cell-Stage Embryos

One-cell-stage rat and mouse zygotes were microinjected by standard procedures. For zebrafish injections, *ubi:eGFP* line from Mosimann lab was used (ubiquitous eGFP expression driven by the *ubiquitin* promoter; see details in Supplemental Information).

T7EI Mutation Detection and Calculation

T7 Endonuclease I (T7EI) assays were performed as previously described (Piganeau et al., 2013) using primers in Table S4.

Sequence modification frequencies were estimated as commonly done: indel rate = $1 - (1 - Xc)^{1/2}$ with Xc, rate of cleaved products and if $Xc < 0.15$, indel rate = Xc/2. For this calculation, the hypothesis is that all heteroduplexes formed during hybridation are cleaved by T7E1. If there is, in addition to wild-type (WT), another homogenous population (X1), as in our KI experiments here, then the previous hypothesis is not appropriate and $X2 = (1 - X1) - (1 - Xc - [X1 \times X1])^{1/2}$ with X2, heterogeneous mutated population and indel rate = X2 + X1. We observed that, when KI rates are higher than T7E1 cleavage rates obtained in the absence of donor, the T7E1 assay was likely not able to cleave all heteroduplexes, especially the ones with the FLAG sequence insertion (that are abundant when KI rates are high), and even using the corrected formula, we underestimated the mutation rates. It is the reason why we chose in these cases to report the rate of T7E1 cleavage and not estimated indel rates.

Evaluation of KI Rates

Integration rates were evaluated by RFLP or PCR. DNA was extracted from transfected cells generally at 6 days after nucleofection. When necessary, nuclease treatment was done before PCR reaction to eliminate residual ODN (see details in Supplemental Information). PCR of the target sites was performed with Phusion polymerase (New England Biolabs). RFLP analysis was performed on 5 μl of the 25 μl PCR reaction and run on 2.5% agarose gels. For analysis of tag insertion, small PCR products spanning the insertion site were resolved on 3% agarose gels and %KI quantified by densitometry measurements of the bands using ImageJ.

TLA

TLA and next-generation sequencing using primers within the ssODNs (see Table S5 and Figure S4A) were used to determine the transgenic ssODNs integration sites as previously described (de Vree et al., 2014).

Amplicon Library Preparation, NGS Sequencing, and Sequence Analysis

DNA was isolated from transfected cells (EZNA tissue kits; Omega Biotek) or zebrafish embryos, and 100–150 ng was added to a 50-μl Phusion polymerase (NEB) reaction. Each sample was assigned a primer set with a unique barcode to enable multiplex sequencing (Table S5). PCR products were purified on a 2% agarose gel, quantified, and pooled into a single sample for sequencing. The single combined sample was treated by the MNHN Genomics Center and sequenced on Ion Torrent PGM. A custom python pipeline was used to count and characterize indels and insert types.

SUPPLEMENTAL INFORMATION

Supplemental Information includes Supplemental Experimental Procedures, five figures, and six tables and can be found with this article online at http://dx.doi.org/10.1016/j.celrep.2016.02.018.

AUTHOR CONTRIBUTIONS

C.G. and J.-P.C. conceived and designed experiments; J.-B.R., C.B., M.C., S.F., A.D.C., L.P., L.T., R.T., S.M., J.E., and N.d.C. performed experiments and did some analyses; J.C. and E.D.-B. wrote the sequence analysis software; C.G., J.-P.C., F.S., Y.C., S.F., A.F., and I.A. analyzed results; and C.G. and J.-P.C. wrote the manuscript with the help of all the authors.

ACKNOWLEDGMENTS

We thank Loïc Ponger and Nicolas Buisine for advice in the development of the software for sequence analysis, Jose Utge and Regis Debruyne for PGM sequencing, Erika Brunet for helpful discussions, genOway's production lab, Wim van Schooten at Cergentis for TLA analysis, and Alain Hilgers for support. This work was supported by ANR Investissement d'Avenir ANR-II-INSB-0014, AFM n°18566, Région Pays de la Loire through Biogenouest, IBiSA program, Fondation Progreffe, and ANR LabCom (project "SOURIRAT"). Sequencing experiments were performed by the integrative genomic facility of Nantes and the SSM department at the Museum National d'Histoire Naturelle in Paris. S.F., Y.C., and A.F. are employees of genOway company.

Received: November 4, 2015
Revised: December 16, 2015
Accepted: January 28, 2016
Published: February 25, 2016

REFERENCES

Bae, S., Kweon, J., Kim, H.S., and Kim, J.S. (2014). Microhomology-based choice of Cas9 nuclease target sites. Nat. Methods *11*, 705–706.

Bedell, V.M., Wang, Y., Campbell, J.M., Poshusta, T.L., Starker, C.G., Krug, R.G., 2nd, Tan, W., Penheiter, S.G., Ma, A.C., Leung, A.Y., et al. (2012). In vivo genome editing using a high-efficiency TALEN system. Nature *491*, 114–118.

Bétermier, M., Bertrand, P., and Lopez, B.S. (2014). Is non-homologous end-joining really an inherently error-prone process? PLoS Genet. *10*, e1004086.

Beumer, K.J., Trautman, J.K., Christian, M., Dahlem, T.J., Lake, C.M., Hawley, R.S., Grunwald, D.J., Voytas, D.F., and Carroll, D. (2013a). Comparing zinc finger nucleases and transcription activator-like effector nucleases for gene targeting in Drosophila. G3 (Bethesda) *3*, 1717–1725.

Beumer, K.J., Trautman, J.K., Mukherjee, K., and Carroll, D. (2013b). Donor DNA utilization during gene targeting with zinc-finger nucleases. G3 (Bethesda) *3*, 657–664.

Branda, C.S., and Dymecki, S.M. (2004). Talking about a revolution: The impact of site-specific recombinases on genetic analyses in mice. Dev. Cell *6*, 7–28.

Carroll, D., and Beumer, K.J. (2014). Genome engineering with TALENs and ZFNs: repair pathways and donor design. Methods *69*, 137–141.

Chen, F., Pruett-Miller, S.M., Huang, Y., Gjoka, M., Duda, K., Taunton, J., Collingwood, T.N., Frodin, M., and Davis, G.D. (2011). High-frequency genome editing using ssDNA oligonucleotides with zinc-finger nucleases. Nat. Methods *8*, 753–755.

Chu, V.T., Weber, T., Wefers, B., Wurst, W., Sander, S., Rajewsky, K., and Kühn, R. (2015). Increasing the efficiency of homology-directed repair for CRISPR-Cas9-induced precise gene editing in mammalian cells. Nat. Biotechnol. *33*, 543–548.

de Vree, P.J., de Wit, E., Yilmaz, M., van de Heijning, M., Klous, P., Verstegen, M.J., Wan, Y., Teunissen, H., Krijger, P.H., Geeven, G., et al. (2014). Targeted sequencing by proximity ligation for comprehensive variant detection and local haplotyping. Nat. Biotechnol. *32*, 1019–1025.

Dorsett, Y., Zhou, Y., Tubbs, A.T., Chen, B.R., Purman, C., Lee, B.S., George, R., Bredemeyer, A.L., Zhao, J.Y., Sodergen, E., et al. (2014). HCoDES reveals chromosomal DNA end structures with single-nucleotide resolution. Mol. Cell *56*, 808–818.

Eckstein, F. (2000). Phosphorothioate oligodeoxynucleotides: what is their origin and what is unique about them? Antisense Nucleic Acid Drug Dev. *10*, 117–121.

Gagnon, J.A., Valen, E., Thyme, S.B., Huang, P., Akhmetova, L., Pauli, A., Montague, T.G., Zimmerman, S., Richter, C., and Schier, A.F. (2014). Efficient mutagenesis by Cas9 protein-mediated oligonucleotide insertion and large-scale assessment of single-guide RNAs. PLoS ONE *9*, e98186.

Harel, I., Benayoun, B.A., Machado, B., Singh, P.P., Hu, C.K., Pech, M.F., Valenzano, D.R., Zhang, E., Sharp, S.C., Artandi, S.E., and Brunet, A. (2015). A

platform for rapid exploration of aging and diseases in a naturally short-lived vertebrate. Cell *160*, 1013–1026.

Hendel, A., Bak, R.O., Clark, J.T., Kennedy, A.B., Ryan, D.E., Roy, S., Steinfeld, I., Lunstad, B.D., Kaiser, R.J., Wilkens, A.B., et al. (2015). Chemically modified guide RNAs enhance CRISPR-Cas genome editing in human primary cells. Nat. Biotechnol. *33*, 985–989.

Hruscha, A., Krawitz, P., Rechenberg, A., Heinrich, V., Hecht, J., Haass, C., and Schmid, B. (2013). Efficient CRISPR/Cas9 genome editing with low off-target effects in zebrafish. Development *140*, 4982–4987.

Hsu, P.D., Lander, E.S., and Zhang, F. (2014). Development and applications of CRISPR-Cas9 for genome engineering. Cell *157*, 1262–1278.

Jepsen, J.S., and Wengel, J. (2004). LNA-antisense rivals siRNA for gene silencing. Curr. Opin. Drug Discov. Devel. *7*, 188–194.

Jinek, M., Chylinski, K., Fonfara, I., Hauer, M., Doudna, J.A., and Charpentier, E. (2012). A programmable dual-RNA-guided DNA endonuclease in adaptive bacterial immunity. Science *337*, 816–821.

Kim, H., and Kim, J.S. (2014). A guide to genome engineering with programmable nucleases. Nat. Rev. Genet. *15*, 321–334.

Kleinstiver, B.P., Prew, M.S., Tsai, S.Q., Topkar, V.V., Nguyen, N.T., Zheng, Z., Gonzales, A.P., Li, Z., Peterson, R.T., Yeh, J.R., et al. (2015). Engineered CRISPR-Cas9 nucleases with altered PAM specificities. Nature *523*, 481–485.

Majumdar, A., Muniandy, P.A., Liu, J., Liu, J.L., Liu, S.T., Cuenoud, B., and Seidman, M.M. (2008). Targeted gene knock in and sequence modulation mediated by a psoralen-linked triplex-forming oligonucleotide. J. Biol. Chem. *283*, 11244–11252.

Nakade, S., Tsubota, T., Sakane, Y., Kume, S., Sakamoto, N., Obara, M., Daimon, T., Sezutsu, H., Yamamoto, T., Sakuma, T., and Suzuki, K.T. (2014). Microhomology-mediated end-joining-dependent integration of donor DNA in cells and animals using TALENs and CRISPR/Cas9. Nat. Commun. *5*, 5560.

Orlando, S.J., Santiago, Y., DeKelver, R.C., Freyvert, Y., Boydston, E.A., Moehle, E.A., Choi, V.M., Gopalan, S.M., Lou, J.F., Li, J., et al. (2010). Zinc-finger nuclease-driven targeted integration into mammalian genomes using donors with limited chromosomal homology. Nucleic Acids Res. *38*, e152.

Paix, A., Wang, Y., Smith, H.E., Lee, C.Y., Calidas, D., Lu, T., Smith, J., Schmidt, H., Krause, M.W., and Seydoux, G. (2014). Scalable and versatile genome editing using linear DNAs with microhomology to Cas9 Sites in Caenorhabditis elegans. Genetics *198*, 1347–1356.

Piganeau, M., Ghezraoui, H., De Cian, A., Guittat, L., Tomishima, M., Perrouault, L., René, O., Katibah, G.E., Zhang, L., Holmes, M.C., et al. (2013). Cancer translocations in human cells induced by zinc finger and TALE nucleases. Genome Res. *23*, 1182–1193.

Porteus, M.H., and Carroll, D. (2005). Gene targeting using zinc finger nucleases. Nat. Biotechnol. *23*, 967–973.

Ran, F.A., Hsu, P.D., Wright, J., Agarwala, V., Scott, D.A., and Zhang, F. (2013). Genome engineering using the CRISPR-Cas9 system. Nat. Protoc. *8*, 2281–2308.

Rios, X., Briggs, A.W., Christodoulou, D., Gorham, J.M., Seidman, J.G., and Church, G.M. (2012). Stable gene targeting in human cells using single-strand oligonucleotides with modified bases. PLoS ONE *7*, e36697.

Sargent, R.G., Kim, S., and Gruenert, D.C. (2011). Oligo/polynucleotide-based gene modification: strategies and therapeutic potential. Oligonucleotides *21*, 55–75.

Shao, Y., Guan, Y., Wang, L., Qiu, Z., Liu, M., Chen, Y., Wu, L., Li, Y., Ma, X., Liu, M., and Li, D. (2014). CRISPR/Cas-mediated genome editing in the rat via direct injection of one-cell embryos. Nat. Protoc. *9*, 2493–2512.

Storici, F., Snipe, J.R., Chan, G.K., Gordenin, D.A., and Resnick, M.A. (2006). Conservative repair of a chromosomal double-strand break by single-strand DNA through two steps of annealing. Mol. Cell. Biol. *26*, 7645–7657.

Tan, W., Carlson, D.F., Lancto, C.A., Garbe, J.R., Webster, D.A., Hackett, P.B., and Fahrenkrug, S.C. (2013). Efficient nonmeiotic allele introgression in livestock using custom endonucleases. Proc. Natl. Acad. Sci. USA *110*, 16526–16531.

Tsai, S.Q., Zheng, Z., Nguyen, N.T., Liebers, M., Topkar, V.V., Thapar, V., Wyvekens, N., Khayter, C., Iafrate, A.J., Le, L.P., et al. (2015). GUIDE-seq enables genome-wide profiling of off-target cleavage by CRISPR-Cas nucleases. Nat. Biotechnol. *33*, 187–197.

Yang, L., Guell, M., Byrne, S., Yang, J.L., De Los Angeles, A., Mali, P., Aach, J., Kim-Kiselak, C., Briggs, A.W., Rios, X., et al. (2013). Optimization of scarless human stem cell genome editing. Nucleic Acids Res. *41*, 9049–9061.

Yang, H., Wang, H., and Jaenisch, R. (2014). Generating genetically modified mice using CRISPR/Cas-mediated genome engineering. Nat. Protoc. *9*, 1956–1968.

Yoshimi, K., Kaneko, T., Voigt, B., and Mashimo, T. (2014). Allele-specific genome editing and correction of disease-associated phenotypes in rats using the CRISPR-Cas platform. Nat. Commun. *5*, 4240.

Zetsche, B., Gootenberg, J.S., Abudayyeh, O.O., Slaymaker, I.M., Makarova, K.S., Essletzbichler, P., Volz, S.E., Joung, J., van der Oost, J., Regev, A., et al. (2015). Cpf1 is a single RNA-guided endonuclease of a class 2 CRISPR-Cas system. Cell *163*, 759–771.